Preprint typeset using LaTeX style emulateapj v. 14/09/00

THE IMPACT OF COOLING AND PRE-HEATING ON THE SUNYAEV–ZEL'DOVICH EFFECT

ANTONIO C. DA SILVA,[1] SCOTT T. KAY,[1] ANDREW R. LIDDLE,[1] PETER A. THOMAS,[1]
FRAZER R. PEARCE[2] AND DOMINGOS BARBOSA[3]
[1]Astronomy Centre, University of Sussex, Brighton BN1 9QJ, United Kingdom
[2]Physics and Astronomy, University of Nottingham, Nottingham NG7 2RD, United Kingdom
[3]Physics Division, Lawrence Berkeley Laboratory, University of California, Berkeley CA, U. S. A.
[4]CENTRA, Instítuto Superior Técnico, Lisboa, Portugal

ABSTRACT

We use hydrodynamical simulations to assess the impact of radiative cooling and 'pre-heating' on predictions for the Sunyaev–Zel'dovich (SZ) effect. Cooling significantly reduces both the mean SZ signal and its angular power spectrum, while pre-heating can give a higher mean distortion while leaving the angular power spectrum below that found in a simulation without heating or cooling. We study the relative contribution from high and low density gas, and find that in the cooling model about 60 per cent of the mean thermal distortion arises from low overdensity gas. We find that haloes dominate the thermal SZ power spectrum in all models, while in the cooling simulation the kinetic SZ power spectrum originates predominantly in lower overdensity gas.

Subject headings: cosmic microwave background – cosmology: theory – galaxies: clusters – methods: numerical

1. INTRODUCTION

One of the most promising techniques for detecting overdense structures at high redshift is from their imprint on the Cosmic Microwave Background (CMB), known as the Sunyaev–Zel'dovich (SZ) effect (Sunyaev & Zel'dovich 1972, 1980). The SZ effect arises due to scattering of the CMB photons from electrons in regions of ionized gas. It has two components, the thermal and kinetic effects (see Birkinshaw 1999 for a review). Successful SZ detections towards known low-redshift galaxy clusters are now routine (e.g. Jones et al. 1993; Myers et al. 1997; Carlstrom et al. 2000) and observational studies are poised to move to blank field surveys of the sky in an attempt to discover their high-redshift counterparts (e.g. Lo et al. 2000; Kneissl et al. 2001). This has led to an upsurge in theoretical work predicting what future surveys might see, the most powerful technique being the use of *N*-body/hydrodynamical simulations to make high-resolution maps (da Silva et al. 2000, 2001; Refregier et al. 2000; Seljak, Burwell & Pen 2001; Springel, White & Hernquist 2001). While these simulations model gravitational collapse, adiabatic compression and shock-heating of the baryons, they ignore the effects of radiative cooling which affects the thermal state of the gas, particularly that in haloes (Pearce et al. 2000; Muanwong et al. 2001) where the SZ signal is strongest. Additionally, it is now believed that the baryons were subjected to non-gravitational heating processes, probably before clusters formed (e.g. Ponman, Cannon & Navarro 1999); such 'pre-heating' could come from the feedback of energy from supernovae or AGN, and is therefore inherently related to the galaxy formation process.

In this Letter, we present a first attempt to simulate the SZ effect using hydrodynamical simulations which implement models for both radiative cooling and pre-heating. While these simulations cannot be regarded as definitive, they illustrate how these processes affect predictions for SZ-related quantities. We focus on the simplest measurable quantities, which are the mean thermal distortion, and the dispersion and angular power spectra of the SZ-induced temperature anisotropies. We also quantify the relative contributions to the SZ effect from bound gas in haloes and the low-overdensity intergalactic medium (IGM).

2. SIMULATION DETAILS AND SZ MAP-MAKING

We present results from three simulations of the currently favoured ΛCDM cosmology. We set the cosmological parameters as follows: matter density, $\Omega_{\rm m} = 0.35$; cosmological constant, $\Omega_\Lambda \equiv \Lambda/3H_0^2 = 0.65$; Hubble constant, $h = H_0/100\,{\rm km\,s^{-1}\,Mpc^{-1}} = 0.71$; baryon density, $\Omega_{\rm B}h^2 = 0.019$; normalization $\sigma_8 = 0.9$. The density field was constructed using $N = 4,096,000$ particles of both baryonic and dark matter, perturbed from a regular grid of fixed comoving size $L = 100\,h^{-1}$Mpc. The dark matter and baryon particle masses are $2.1 \times 10^{10}\,h^{-1}{\rm M}_\odot$ and $2.6 \times 10^{9}\,h^{-1}{\rm M}_\odot$ respectively. In physical units, the gravitational softening was held fixed to $25\,h^{-1}$kpc below $z = 1$ and above this redshift scaled as $50(1+z)^{-1}\,h^{-1}$kpc. Each simulation took approximately 2300 time steps to evolve to $z = 0$, using a parallel version of the HYDRA code (Couchman, Thomas & Pearce 1995; Pearce & Couchman 1997), which uses the adaptive particle-particle/particle-mesh ($\rm AP^3M$) algorithm to calculate gravitational forces (Couchman 1991) and smoothed particle hydrodynamics (SPH) to estimate hydrodynamical quantities. Our SPH implementation follows that used by Thacker & Couchman (2000), where more details can be found.

The first of the three simulations was performed without any additional heating or cooling mechanisms; we refer to this as the 'non-radiative' simulation. The second simulation included a model for radiative cooling using the method described in Thomas & Couchman (1992), except that we adopted the cooling tables of Sutherland & Dopita (1993) and a global gas metallicity evolving as $Z = 0.3(t/t_0)Z_\odot$, where $t_0 \simeq 12.8\,$Gyr is the current age of the Universe. Cooled gas is converted into collisionless material and no longer participates in generating the SZ effect. This fraction is negligible at $z = 6.5$ (the highest redshift we consider in computing the SZ effect) but increases to ~ 20 per cent by the present. Although this model provides acceptable matches to the $z = 0$ X-ray group/cluster scaling relations (Muanwong et al. 2001), the fraction of cooled material is uncomfortably high when compared to observational determinations (e.g. Balogh et al. 2001). Hence, this simulation provides an extreme case in terms of the amount of cooling obtained.

Our third simulation, which also includes cooling, was performed in order to study the effects of pre-heating the gas at

high redshift. Although attempts are now being made to include effective energy feedback from supernovae within cosmological simulations (e.g. Kay et al. 2001), the modelling can only be done at a phenomenological level since the true physical processes occur on much smaller scales than are resolved. For the purposes of this paper, we adopt a particularly simple model, which is to take the output from the radiative simulation at $z = 4$ and raise the specific thermal energy of all gas particles by 0.1 keV (an equivalent temperature of 1.2×10^6 K), before evolving to $z = 0$ as before. This choice of energy is motivated by observations of an 'entropy floor' in X-ray groups by Lloyd-Davies, Ponman & Cannon (2000); we define specific 'entropy' as $s = k_B T/n^{2/3}$ and our injection model would give $s_{\rm floor} \sim 80\,{\rm keV\,cm^2}$ were the gas all at mean density. This reduces the amount of cooled material to a more acceptable level ($\sim 10\%$), although a greater amount of heating would have been needed to give the best match to the X-ray scaling relations.

These simulations have two advantages over those we studied previously (da Silva et al. 2000, 2001). Firstly, those simulations did not include radiative cooling, and so contain hot high-density gas where the cooling time is much shorter than a Hubble time. Secondly, the new simulations have improved numerical resolution (the particle masses are a factor of 19 smaller) allowing the SZ effect to be studied at smaller scales.

We analyze the SZ effect by constructing simulated SZ maps of area one square degree,[1] stacking simulation boxes from low to high redshift (up to redshift $z \sim 6.5$) as described by da Silva et al. (2000). The vast majority of the thermal SZ signal is produced well within this redshift interval. We repeat this process to produce 30 random map realizations for each run, using the same sequence of random seeds for the different models. The thermal effect is described by the Comptonization parameter y, and the kinetic by the temperature perturbation $\Delta T/T$.

3. RESULTS

3.1. *The mean thermal distortion and the rms dispersion*

The mean y distortion, obtained by averaging y over lines of sight, is an important measure of the global state of the gas in the Universe. In our simulations we find

Non-radiative:	$y_{\rm mean} = 3.2 \times 10^{-6}$
Cooling:	$y_{\rm mean} = 2.3 \times 10^{-6}$
Pre-heating:	$y_{\rm mean} = 4.6 \times 10^{-6}$.

(For comparison, the mean mass-weighted temperature at $z = 0$ in the three simulations are 0.39, 0.35 and 0.38 keV.) At present, the best upper limit is $y_{\rm mean} < 1.5 \times 10^{-5}$ from *COBE–FIRAS* (Fixsen et al. 1996), and all our models are well below this. The cooling simulation gives the lowest level of distortion and the pre-heating the highest. The factor of two difference between these runs shows that the mean y is quite sensitive to pre-heating. The mean y distortion in the non-radiative model is slightly smaller than the value found in da Silva et al. (2000); part of this difference is attributable to a different σ_8, and the remainder lies within the uncertainty expected from changes to the simulation technique.

To study the relative contribution to the SZ effect from the different gas phases in the simulations, we sorted the particles in each simulation according to their temperature, T, and overdensity, δ, and computed the fraction of SZ signal arising from

[1] A collection of colour images and animations can be viewed at `www.astronomy.sussex.ac.uk/users/antonio/sz.html`

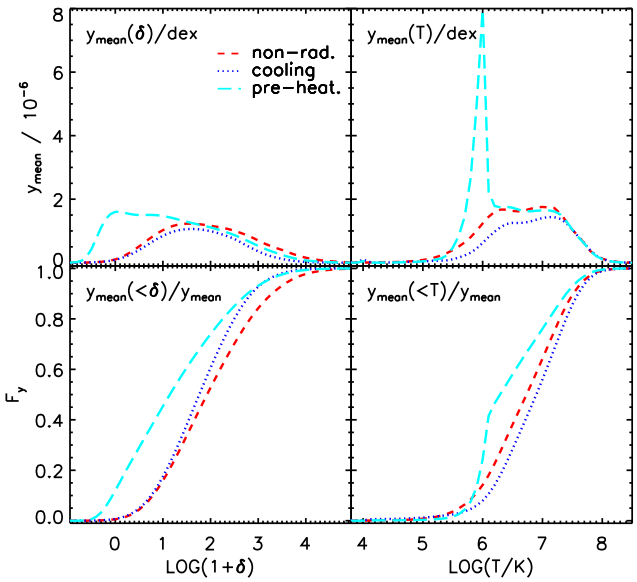

FIG. 1.— Fractional contribution to $y_{\rm mean}$ as a function of temperature and overdensity. The upper panels show the contribution for a unit interval (in base ten logarithm), while the lower show the integrated contribution.

all particles at a given T and δ. By carrying out cuts in the δ–T plane we are able to determine the type of structures contributing to the SZ effect. In Figure 1, the top panels show the distribution of the mean y as a function of overdensity and temperature. The area under the curves are the $y_{\rm mean}$ listed earlier. The bottom panels show the corresponding cumulative mean y fractions, $F_y = y_{\rm mean}(<\delta)/y_{\rm mean}$ and $F_y = y_{\rm mean}(<T)/y_{\rm mean}$.

The left-hand panels show that the mean y receives contributions from a wide range of overdensities. Cooling reduces the contribution from high-density gas in groups and clusters. Because most of the gas in the simulations is at low overdensity, pre-heating preferentially raises the contribution from that phase. The right-hand panels in Figure 1 indicate that gas below 10^5K and above 10^8K contributes negligibly to $y_{\rm mean}$. The mean y distributions have similar shapes in the cooling and non-radiative models and are practically uniform in the range $6.2 \lesssim \log(T/{\rm K}) \lesssim 7.3$ for all runs. Gas above $\sim 2 \times 10^7$K produces the same amount of distortion independently of the model considered. The pre-heating run shows a sharp peak at $T \simeq 10^6$K resulting from IGM gas heated to this temperature by the energy injection at $z = 4$. While pre-heating will indeed insert a new temperature scale, the narrowness of this feature is no doubt an artifact of our simplified method and would be broadened in reality. Indeed, there is evidence that some of the IGM is cooler than this (Schaye et al. 2000).

Figure 2 shows the rms temperature perturbation $\sigma_{\rm rms}$ as a function of beam resolution $\theta_{\rm FWHM}$, obtained by averaging the 30 thermal (Rayleigh–Jeans band) and kinetic SZ maps. The different cooling/pre-heating models shift the curves by tens of percent. On the angular scales shown, the kinetic dispersions are a factor $\sim$5 smaller than the thermal, confirming earlier results using lower-resolution simulations (da Silva et al. 2001).

3.2. *The angular power spectra*

Figure 3 shows the SZ angular power spectra in the Rayleigh–Jeans region, with C_ℓ defined in the usual way. In each case,

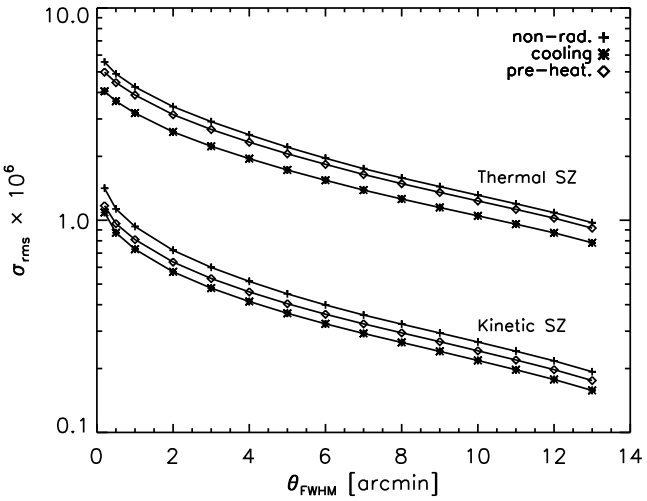

FIG. 2.— Dispersion $\sigma_{\rm rms}$ for the thermal and kinetic effects, as a function of beam resolution (assuming gaussian beams with FWHM=$\theta_{\rm FWHM}$).

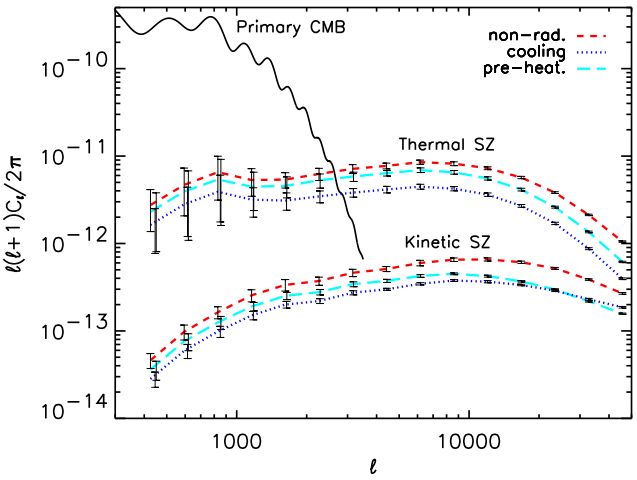

FIG. 3.— Thermal and kinetic angular power spectra from the three simulations. Curves are averages over 30 maps and bars are 1σ bootstrap errors.

the curves show averages over 30 sky realizations, and the error bars are statistical errors at 68 per cent confidence level obtained by bootstrap resampling the set of maps. The map-to-map variations are typically much higher than these and in particular, as we will see below, the large angular scales are significantly affected by sample variance as well as the finite map size. Comparing the different models, we see that the curves have similar shapes, with the thermal power spectra dominating the kinetic ones on all scales, and dominating the primary CMB anisotropies for $\ell > 3000$. Radiative cooling has the effect of lowering the SZ spectra by a factor of about two as compared with the non-radiative case. Our model of pre-heating raises the spectra again, though only part way back towards those found in the non-radiative run.

Figure 4 shows the contributions to the power spectra from the low-overdensity IGM ($\delta < 100$) and from bound gas in haloes ($\delta > 100$). Most of the thermal signal comes from the

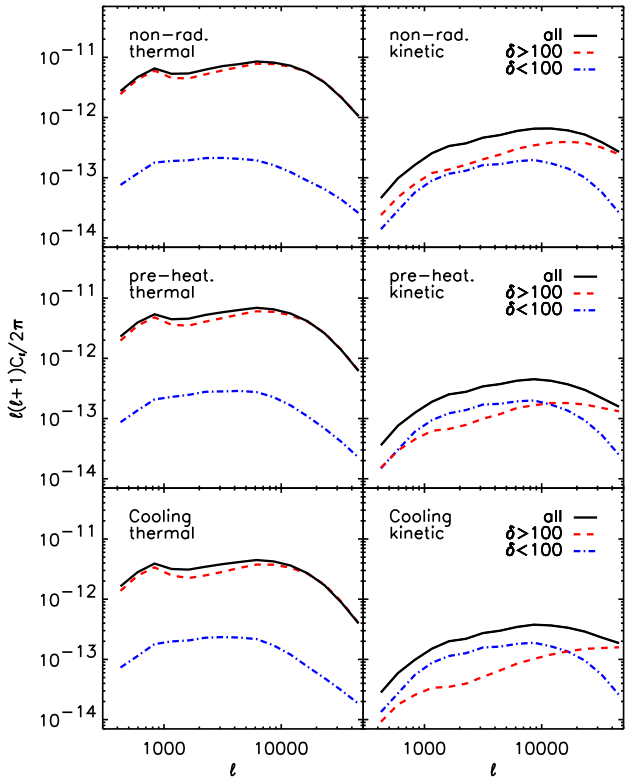

FIG. 4.— Contribution to the spectra from gas in haloes ($\delta > 100$) and the low-overdensity intergalactic medium ($\delta < 100$).

bound gas, with the IGM contribution an order of magnitude below. The kinetic signal is dominated by halos in the non-radiative run, by the IGM phase in the cooling simulation, and has roughly equal contributions from each in the pre-heating model. Accordingly, treatments of the kinetic effect which concentrate solely on bound haloes are likely to miss much of the kinetic signal. For both the thermal and kinetic effects, the contribution from low-density gas is similar in all three models, and the difference in the spectral amplitudes is therefore mainly due to the contribution of the high-density gas. These differences mainly reflect the different amounts of cooled material in haloes in each simulation. At $z = 0$ the amount of cooled material in the pre-heating run is a factor of about two less than in the cooling simulation (while the non-radiative model does not include star formation at all).

We end by discussing how cosmic variance and numerical resolution affects these determinations. Even though our spectra are averages over 30 maps, there remains some sensitivity to rare features, and because these are nongaussian they can have large effects, as reflected in the bootstrap errors. One of the 30 thermal maps is dominated by a very nearby bright source, strong enough to greatly boost the estimated power spectrum. In Figure 5 the solid line reproduces the mean power spectrum from Figure 3, while the dashed line shows the median power spectrum, which is close to what would have been obtained had a single map with a bright source by chance not appeared in the set. The median is consistent with the bootstrap errors (which of course include subsamples without that map); note however that it is the mean, not the median, which is the max-

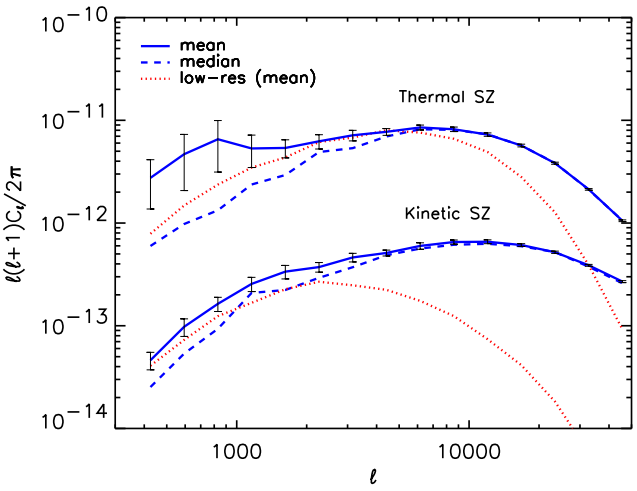

FIG. 5.— Effects of sample variance and resolution on the SZ spectra obtained from non-radiative simulations. The curves are the mean power spectra (solid lines) and the median of the C_l distributions (dashed lines). The mean power spectra from da Silva et al. (2001) are shown as the dotted lines.

imum likelihood power spectrum estimator. We conclude that there is considerable sample variance error in estimating the thermal power spectrum from observations with limited survey areas. The dotted lines show the SZ power spectra obtained from the non-radiative ΛCDM simulation studied in da Silva et al. (2001), which had a mass resolution 19 times worse than the present simulations. The loss of power due to resolution in the earlier results is clearly seen at high ℓ, an effect particularly severe in the kinetic case, and our new results extend the ℓ-range for which the power spectra are reliably obtained. Based on the demonstrated convergence of the low-resolution simulations, we estimate the thermal power spectrum is accurately determined out to at least ℓ of 20,000.

Our non-radiative SZ angular power spectra show broad agreement with the results obtained by other authors, who use only non-radiative hydrodynamical simulations. After accounting for the differing σ_8 and $\Omega_{\rm B}h$, on large scales our mean thermal spectrum agrees well with the results of Refregier et al. (2000) and Refregier & Teyssier (2000), whereas the predictions from Seljak et al. (2000) and Springel et al. (2000) are closer to our median C_ℓs. On small scales our mean thermal spectrum shows somewhat less power and a similar shape to the results in Springel et al. (2000) and Refregier & Teyssier (2000), while our kinetic angular power spectrum is in good agreement with that of Springel et al. (2000).

4. CONCLUSIONS

We have analyzed the impact on the magnitude and spectrum of the SZ effect of physical processes in the hot gas, including both radiative cooling and a crude model for pre-heating of the IGM. While neither radically alters the appearance of the SZ sky, the details of how the signal is generated are modified. Cooling reduces the angular power spectrum by a factor of around two as compared to non-radiative simulations, while our pre-heating model gives a significant boost to the mean distortion but a more minor change to the power spectra.

We have studied these effects in more detail by classifying the gas into two phases. While the mean thermal distortion receives equal contribution from gas in haloes and the IGM, the thermal angular power spectrum is dominated by contributions from hot gravitationally-bound gas. By contrast, the kinetic power spectrum receives equal contributions from both phases in the pre-heating run and is dominated by the IGM in the cooling model. For both the thermal and kinetic SZ spectra, the contribution from IGM gas is similar in all three models, whereas the contribution from gas in haloes is largest in the non-radiative simulation and lowest in the cooling run.

ACdS and DB were supported by FCT (Portugal), and STK, PAT and FRP by PPARC (UK). The work presented in this paper was carried out as part of the programme of the Virgo Supercomputing Consortium (`www.virgo.sussex.ac.uk`).

REFERENCES

Balogh M. L., Pearce F. R., Bower R. G., Kay S. T., 2001, MNRAS, 326, 1228
Birkinshaw M., 1999, Phys. Rep., 310, 98
Carlstrom J. A., Joy M. K., Grego L., Holder G. P., Holzapfel L., Mohr J. J., Patel S., Reese E. D., 2000, Physica Scripta, T85, 148
Couchman H. M. P., 1991, ApJ, 368, L23
Couchman H. M. P., Thomas P. A., Pearce F. R., 1995, MNRAS, 452, 797
da Silva A. C., Barbosa D., Liddle A. R., Thomas P. A., 2000, MNRAS, 317, 37
da Silva A. C., Barbosa D., Liddle A. R., Thomas P. A., 2001, MNRAS, 326, 155
Fixsen D. J., Cheng E. S., Gales J. M., Mather J. C., Shafer R. A., Wright E. L., 1996, ApJ, 473, 576
Jones M. et al., 1993, Nature 365, 320
Kay S. T., Pearce F. R., Frenk C. S., Jenkins A., 2001, astro-ph/0106462
Kneissl R., Jones M., Saunders R., Eke V., Lasenby A., Grainge K., Cotter G., 2001, astro-ph/0103042
Lloyd–Davies E. J., Ponman T. J., Cannon D. B., 2000, MNRAS, 315, 689
Lo K., Chiueh T., Martin R., Ng Kin-Wang, Liang H., Pen U.-L., Ma C.-P., 2000, astro-ph/0012282
Muanwong O., Thomas P. A., Kay S. T., Pearce F. R., Couchman H. M. P., 2001, ApJ, 552, L27
Myers S. T., Baker J. E., Readhead S. A. G., Leitch E. M., Herbig T., 1997, ApJ, 485, 1
Pearce F. R., Couchman H. M. P., 1997, New Astronomy, 2, 411
Pearce F. R., Thomas P. A., Couchman H. M. P., Edge A. C., 2000, MNRAS, 317, 1029
Ponman T. J., Cannon D. B., Navarro J. F., 1999, Nature, 397, 135
Refregier A., Komatsu E., Spergel D., Pen U.-L., 2000, Phys. Rev. D, 61, 123001
Refregier A., Teyssier R., 2000, astro-ph/0012086
Schaye J., Theuns T., Rauch M., Efstathiou G., Sargent W., 2000, MNRAS, 318, 817
Seljak U., Burwell J., Pen U.-L., 2001, Phys. Rev. D, 63, 063001
Springel V., White M., Hernquist L., 2001, ApJ, 549, 681
Sunyaev R. A., Zel'dovich Ya. B., 1972, Comm. Astrophys. Space Phys., 4, 173
Sunyaev R. A., Zel'dovich Ya. B., 1980, ARA&A, 18, 537
Sutherland R. S., Dopita M. A., 1993, ApJS, 88, 253
Thacker R. J., Couchman H. M. P., 2000, ApJ, 545, 728
Thomas P. A., Couchman H. M. P., 1992, MNRAS, 257, 11